



Multiscale NMR and relaxation / RMN et relaxation multi-échelles

## One- and two-dimensional spin correlation of complex fluids and the relation to fluid composition

*Corrélations de spin à une et deux dimensions dans les fluides complexes reliées à leurs compositions*

Denise E. Freed, Martin D. Hürlimann\*

Schlumberger-Doll Research, One Hampshire Street, Cambridge, MA 02139, USA

## ARTICLE INFO

## Article history:

Available online 27 July 2010

## Keywords:

Complex fluids  
Crude oils  
Low field relaxation  
Diffusion  
Inverse Laplace transform  
Fluid composition  
Scaling

## Mots-clés:

Fluides complexes  
Huiles lourdes  
Relaxation à bas champ  
Diffusion  
Transformée de Laplace Inverse  
Composition de fluide  
«Scaling»

## ABSTRACT

Many natural fluids, including crude oils, are complex mixtures of molecules with a broad range of sizes and chemical properties. In such systems, the molecular dynamics is complex and the relaxation and diffusion behavior cannot be described by a single relaxation time or diffusion coefficient. Nevertheless, low field NMR relaxation and diffusion measurements have become powerful tools for the study of such fluids. The complexity can be overcome by analyzing the measurements in terms of one- and two-dimensional distribution functions. The one-dimensional relaxation and diffusion distribution functions are directly related to the composition of the fluids. We also show that from the analysis of the shape of the relaxation and diffusion decay, it is possible to predict the temperature dependence of viscosity. Two-dimensional distribution functions probe further aspects of the molecular dynamics. The correlation between  $T_1$  and  $T_2$  relaxation behavior can be used to detect the presence of slow motion and to probe the aggregation of molecules into supermolecular structures. Diffusion-relaxation distribution functions give information about the chemical composition of the fluid.

© 2010 Académie des sciences. Published by Elsevier Masson SAS. All rights reserved.

## R É S U M É

Beaucoup de fluides naturels, en particulier les huiles lourdes, sont des mélanges complexes de molécules possédant une large distribution de tailles et de propriétés chimiques. Dans ces systèmes, la dynamique des molécules est complexe et le comportement de relaxation et de diffusion ne peut pas se décrire par un simple temps de relaxation ou coefficient de diffusion. Néanmoins, la relaxation RMN à bas champ et les mesures de diffusion sont devenus des outils puissants pour étudier de tels fluides. On peut contourner la complexité en analysant les mesures en termes de fonctions de distributions à une et deux dimensions. Les fonctions de distribution de relaxation et de diffusion à une dimension sont directement reliées à la composition des fluides. On montre également que l'analyse de la forme des déclin de relaxation et de diffusion permet de prédire la dépendance en température de la viscosité. Les fonctions de distribution à deux dimensions permettent de suivre d'autres aspects de la dynamique moléculaire. Les corrélations entre les comportements de relaxation  $T_1$  et  $T_2$  peuvent être utilisés pour détecter des mouvements lents et mettre en évidence l'agrégation des molécules en structures supramoléculaires. Les corrélations entre les fonctions de distribution de

\* Corresponding author.

E-mail address: [hurlimann@slb.com](mailto:hurlimann@slb.com) (M.D. Hürlimann).

diffusion et de relaxation donnent enfin des informations sur la composition chimique des fluides étudiés.

© 2010 Académie des sciences. Published by Elsevier Masson SAS. All rights reserved.

## 1. Introduction

It is well known that nuclear magnetic relaxation (NMR) measurements can be used to infer the composition of pure fluids [1,2]. Here we focus on one- and two-dimensional spin correlation functions extracted from low field relaxometry and diffusometry data and show how they can be used for the characterization of complex fluids and their composition. The relaxation behavior of such systems cannot be described by a single relaxation time and it is important to analyze the full shape of the relaxation decay curve. More generally, it is possible to measure multi-dimensional distribution functions from which we can infer details of the composition and detect aggregation in the fluid.

The composition of naturally occurring fluids is often very complex. Examples include many biological fluids and the fluids filling the pore space of geological formations, in particular crude oils. Such fluids typically consist of a complex mixture of different molecules with a wide range of sizes and chemical properties. The molecular composition controls important fluid properties such as the boiling point, vapor pressure, viscosity and phase behavior. In many cases, a subset of the molecules spontaneously aggregate and form supermolecular structures, resulting in a rich phase diagram.

There are a number of widely used analytical techniques for the analysis of complex fluids and the determination of their composition. They include chromatography [3] and mass spectroscopy [4], two techniques that are intrinsically separation techniques. They separate the different molecular entities either with the help of a carrier fluid (liquid or gas) or by first ionizing the molecules and then separating the components using electromagnetic fields. In fluids with a large range of molecular sizes, such as crude oils, it is difficult to obtain quantitative composition results with these techniques over the whole range of molecular sizes. In gas chromatography, large molecules (e.g. molecules with more than about 36 carbon atoms) cannot be easily brought into the gas phase and are therefore not detected. Asphaltene and resins are large molecules in crude oil that play a critical role in determining its behavior. They cannot be characterized with gas chromatography. Mass spectroscopy does not suffer from this particular limitation and also has an unprecedented resolution over a very wide range of atomic sizes. It is an excellent technique for detecting the presence of a particular molecule. However since the efficiency of ionization can vary widely between the molecules (certain classes of molecules might be completely invisible), the method generally cannot quantify the amounts accurately. Furthermore, there are a number of applications where it is essential that the measurements be performed non-invasively. Analytic methods based on separation techniques are not suitable for this purpose.

In such cases, spectroscopic techniques, including optical and NMR spectroscopies, are better suited techniques. However, optical spectroscopic techniques are of limited use with opaque samples such as crude oils. NMR spectroscopy has been developed into an exceedingly powerful technique to analyze the structure of complex molecules in the liquid state [5]. It requires samples of high purity, i.e. a pure substance of interest dissolved in a solvent. When a mixture of molecules is present, the superposition of the spectra from the individual molecules quickly becomes unresolvable as the complexity of the overall NMR spectrum rapidly diverges. This makes NMR spectroscopy unsuitable for the analysis of complex fluids. We discuss here the role of low field NMR relaxometry and diffusometry as techniques for probing the composition of complex fluids.

## 2. Low field NMR relaxation measurements

Relaxation is typically dominated by intramolecular nuclear dipole interactions that are modulated by molecular motions. Longitudinal relaxation measurements are sensitive to the components of the resulting fluctuations  $J(\omega)$  at  $\omega_L$  and  $2\omega_L$ , where  $\omega_L$  is the Larmor frequency [6]. Transverse relaxation is also sensitive to slower fluctuations with frequency close to 0. By performing NMR relaxation measurements in modest magnetic fields that correspond to Larmor frequencies in the range of a few MHz, we probe the low frequency part of the noise spectrum  $J(\omega)$ . For samples that do not show any aggregation, the slowest molecular motions are expected to be associated with the overall tumbling and reorientation of molecules. For a molecule of radius of gyration  $r_g$  in a fluid of viscosity  $\eta$ , we can estimate the tumbling rate by

$$\frac{1}{\tau_R} = \frac{3kT}{4\pi\eta r_g^3} \quad (1)$$

The viscosity of the sample is a collective property and determined by the overall composition of the fluid. According to Eq. (1), the characteristic tumbling rate  $1/\tau_R$  in fluids of low to moderate viscosity (i.e.  $\eta < 100$  cP) is higher than 100 MHz, even for large molecules with a radius of gyration as large as 0.3 nm. This implies that the noise spectrum  $J(\omega)$  has no frequency dependence below 100 MHz and that  $T_1$  and  $T_2$  relaxation measurements at low field, corresponding to Larmor frequencies of a few MHz, provide identical results. On the other hand, if  $T_1$  and  $T_2$  relaxation differ at low fields, then this indicates that there are slower motions than given by Eq. (1) with molecular sizes. This can occur if some of the molecules in the fluid aggregate and form supermolecular structures. Tumbling of such large structures generates

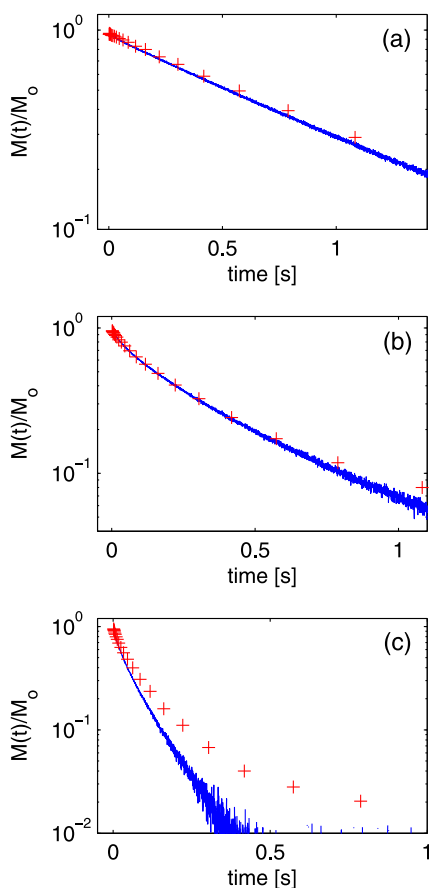


**Fig. 1.** Comparison of  $T_1$  and  $T_2$  decay measured in three different crude oils at a Larmor frequency of 1.76 MHz. The solid lines show the decay of the transverse magnetization  $M_{\perp}(t)$ , normalized by the initial magnetization  $M_0$ . The crosses show  $M_z(t) - M_0$  normalized by  $M_z(0) - M_0$ , which is the normalized deviation of the longitudinal magnetization from the thermal equilibrium. In oils #1 and #2 shown in panels (a) and (b), the transverse and longitudinal relaxation properties are identical, indicating motional averaging and that the spectral densities have no frequency dependence below the Larmor frequency. In contrast, oil #3 in panel (c) shows  $T_1$  behavior that clearly differs from its  $T_2$  behavior. This is caused by the presence of asphaltene aggregates that introduce slow fluctuations to the molecular dynamics.

slow fluctuations, which then leads to  $T_1 > T_2$ . The presence of slow fluctuations can also be detected by measuring the frequency dependence for  $T_1$  relaxation by field cycling relaxometry [7].

In Fig. 1, we present a comparison of  $T_1$  and  $T_2$  measurements at low fields for three different oils. In oils #1 and #2 of Fig. 1, the behavior of  $T_1$  and  $T_2$  relaxation is identical, thus indicating that all molecular motions are fast compared to the Larmor frequency. This is in contrast to oil #3 shown at the bottom. This oil contains asphaltene molecules that aggregate to structures with sizes larger than those of individual molecules. The tumbling of these structures gives rise to the slow fluctuations responsible for  $T_2$  relaxation that is faster than  $T_1$  relaxation.

### 3. Distribution functions

The relaxation behaviors shown in Fig. 1 generally deviate from a single-exponential decay, even in oils with identical  $T_1$  and  $T_2$  behavior (i.e. oils without any asphaltene molecules). In these oils, all spins are in the fast motion regime, but different spins generally relax with different rates. Small molecules tumble faster than large molecules and average out the residual dipolar interaction to a higher degree. As a consequence, spins on small molecules generally relax more slowly than spins on large molecules.

It is therefore natural to describe the total signal as a superposition of contributions from individual spins, where each component decays exponentially with time. For  $T_2$  decay, the magnetization decay is written as

$$M(t) = \int dT_2 f(T_2) \exp\{-t/T_2\} \quad (2)$$

Here  $f(T_2)$  is the one-dimensional distribution function and  $f(T_2)dT_2$  describes the fraction of spins with relaxation times in the range  $T_2 \pm \frac{1}{2}dT_2$ . The distribution function can be extracted from the magnetization decay  $M(t)$  by performing

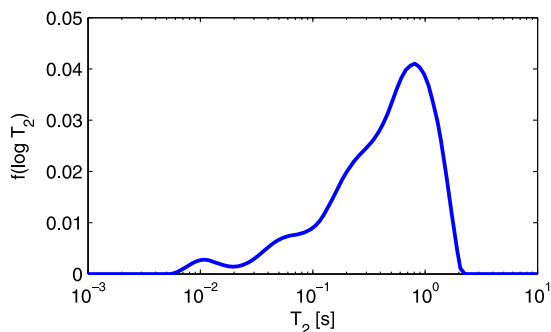


**Fig. 2.** Example of a one-dimensional distribution function  $f(\log T_2)$  extracted from the magnetization decay  $M(t)$  measured on an oil.

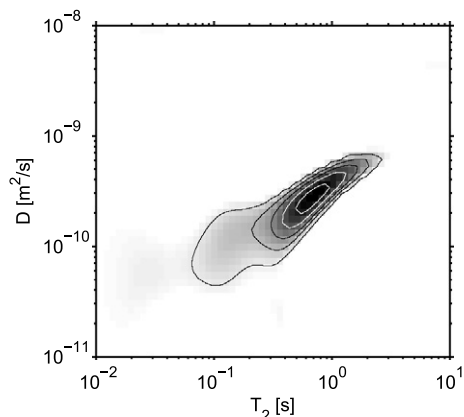


**Fig. 3.** Example of a two-dimensional distribution function  $f(\log D, \log T_2)$  for an oil.

an inverse Laplace transformation [8]. In many cases, the relevant range of  $T_2$  extends over several orders of magnitude. In such cases, it is often more appropriate to extract the distribution function for the variable  $\log T_2$  rather than for  $T_2$ . The distribution functions  $f(T_2)$  and  $f(\log T_2)$  are simply related by  $f(\log T_2) = T_2 f(T_2)$ . An example of the distribution function  $f(\log T_2)$  extracted from the measured relaxation decay  $M(t)$  is given in Fig. 2.

In addition to  $f(T_2)$ , other distribution functions can be measured at low magnetic fields, including  $f(T_1)$  and  $f(D)$ , the one-dimensional distribution functions for longitudinal relaxation or diffusion, respectively. More recently, the methodology has been developed to measure multi-dimensional distribution functions. In particular, two-dimensional distribution functions  $f(T_1, T_2)$  [9] and  $f(D, T_2)$  [10] have proven to be particularly useful for the characterization of complex fluids. An example of  $f(\log D, \log T_2)$  is shown in Fig. 3.

The extraction of these distribution functions is based on inverse Laplace transformations [11]. This mathematical operation requires special care and poses some extra challenges compared to the more common Fourier transform. The inverse Laplace transform is generally ill-conditioned and, as a consequence, there exist many different distribution functions  $f(T_2)$  that fit the data within experimental error [12]. These possible distribution functions have the same overall features, but differ in details at a finer scale of  $T_2$ . We follow here the common practice of presenting only a single ‘representative’ solution. The goal is to find the particular solution that is the smoothest function with the fewest features among all possible solutions of  $f(T_2)$ . It can be obtained by including a regularization term in the inversion. For further details, we refer the reader to the extensive literature on this subject [13].

#### 4. Theory of relaxation and diffusion of complex mixtures

In order to relate the various distribution functions to fluid properties, we review next the theory that describes the connection between fluid composition and the quantities that can be directly measured with low field NMR, i.e. relaxation or diffusion.

##### 4.1. Diffusion coefficient

In a fluid mixture, small molecules generally diffuse faster than large ones. Each molecule can be characterized by an individual diffusion coefficient,  $D_i$ , that quantifies the rate at which its mean-squared displacement increases with time due to Brownian motion. Since we are considering here displacements over distances that are much larger than typical molecular sizes, it is sufficient to analyze only the motion of the center of mass of the molecules. Internal motions average out. As a consequence, all spins on a given molecule have identical diffusion coefficients.

The diffusion property of a mixture is then described by a distribution of individual diffusion coefficients. The individual diffusion coefficient for a given molecule depends on its molecular size and also on the viscosity of the sample. The viscosity is a property that is determined by the overall composition of the fluid and reflects the fluid environment common to all molecules.

The general relation between diffusion and composition is already apparent in the Einstein–Stokes relation. For a hard sphere of radius  $r$  in a solvent of viscosity  $\eta$ , the diffusion coefficient of the sphere is given by

$$D_s = \frac{kT}{6\pi\eta r} \quad (3)$$

This expression is applicable strictly only for spherical particles that are dilute and much larger than the solvent molecules. When the spheres are deformed or the size of the particles are decreased to molecular sizes, it has been found that the

relation between diffusion coefficient and particle size has still the general form of Eq. (3), but with extra factors in the denominator that reflect the microviscosity and the particular shape of the molecule. For molecules with internal degrees of freedom,  $r$  has to be replaced by the radius of gyration.

For multi-component systems, the analysis of diffusion in alkane mixtures [14] has shown that the expression for  $D_i$  can still be factored into two terms. The first term, denoted  $g$ , is inversely proportional to the microviscosity experienced by a monomer of the alkane chain. As long as all molecules are composed of the same monomers, this term is identical for all molecules within the mixture. It depends on the fluid composition only through the average chain length  $\bar{N}$  within the mixture, i.e. its composition dependence can be written as  $g(\bar{N})$ . The second term is molecule specific and depends mainly on the radius of gyration, but also somewhat on the shape and stiffness of the particular component of interest. For mixtures of alkanes that have a wide range of chain length  $N$ , it was found that this second term follows a power law in  $N$  [14]. The diffusion coefficient  $D_i$  for component  $i$  associated with chain length  $N_i$  can then be written as

$$D_i = g(\bar{N})N_i^{-\nu} \quad (4)$$

where for alkane mixtures, the exponent  $\nu \approx 0.7$ . The power-law dependence of the radius of gyration on chain length holds for  $N_i > 2$ . For smaller molecules, corrections have to be applied as discussed in [14].

The internal viscosity function  $g(\bar{N})$  is controlled by the relative free volume, and for mixtures of homologous chains, depends on the fluid composition only through the average chain length  $\bar{N}$ . For mixtures of alkanes,  $g(\bar{N})$  also follows a power law

$$g(\bar{N}) = A\bar{N}^{-\beta} \quad (5)$$

This leads to the general scaling relation between the diffusion coefficient and the composition:

$$D_i = A\bar{N}^{-\beta}N_i^{-\nu} \quad (6)$$

For mixtures of alkanes at room temperature and atmospheric pressure, the exponent  $\beta \approx 1.73$  and the prefactor  $A = 3.5 \times 10^{-7} \text{ m}^2/\text{s}$  [14].

#### 4.2. Relaxation

The theoretical treatment of relaxation is more complicated than that of diffusion because internal motion can contribute to relaxation. Nevertheless, we expect that at low frequencies, the relaxation time for a spin on a given molecule,  $T_{2,i}$ , is primarily determined by the overall tumbling of the molecule, which is typically the slowest motion. For this reason, the relaxation time  $T_{2,i}$ , similar to the diffusion coefficient, is mainly a function of the size of the molecule and the overall viscosity of the fluid. This implies that all spins on the same molecules have comparable relaxation times. This conclusion can be tested by inspecting two-dimensional diffusion–relaxation distribution functions  $f(D, T_2)$  such as that shown in Fig. 3. The measured distribution functions  $f(D, T_2)$  generally show a strong correlation between the diffusion coefficients and relaxation times of a component. For a given diffusion coefficient, the range of relaxation times is fairly narrow. Since different spins on the same molecule have identical diffusion coefficients, it follows that they must also have similar relaxation times.

Given the translational diffusion coefficient, Eq. (4), and assuming that there are hydrodynamic interactions [15,16], then the rotational correlation time  $\tau_{Ri}$  of the  $i$ -th component has the form

$$\frac{1}{\tau_{Ri}} \propto N_i^{-3\nu} g(\bar{N}) \quad (7)$$

As argued above, the relaxation time of the  $i$ -th component,  $T_{2,i}$ , is mainly controlled by  $\tau_{Ri}$ , but it is also affected by internal modes and possibly also by intermolecular interactions. According to [17], the intramolecular interactions play the dominant role in relaxation, although the intermolecular interactions do have some measurable effect. In [16] it was also found that these intermolecular interactions do not have much of an influence on the chain-length dependence of the relaxation times.

In [16], following ideas in [18], the correlation function for the motion of an alkane chain  $i$  was approximated as a product of three different terms,  $G_i(t) = G_{A,i}(t)G_{B,i}(t)G_{C,i}(t)$ , corresponding to three types of motion on three different time scales. The fastest motion is on a very short time scale associated with internal vibrations. The second type at intermediate times describes motion of segments within the molecule, and the third type is due to the overall rotation of molecules, characterized by the time scale  $\tau_{R,i}$ . The very short time-scale motion is local and anisotropic. It has a correlation function that quickly decays to a constant  $G_{A,i} \rightarrow C$  that is independent of chain length. The intermediate time-scale motion is highly correlated and thus takes a long time to lose coherence. In polymer melts, this motion has been analyzed in terms of confinement within an effective tube or as one-dimensional diffusion or crankshaft motion with a correlation function  $G_{B,i}(t)$  that decays to zero via a power law. At long times, this correlation function for component  $i$  is given by

$$G_{B,i}(t) \propto (\tau_{m,i}/t)^{\frac{1}{2}} \quad (8)$$

The characteristic time  $\tau_{m,i}$  may have some weak chain length dependence, and it typically depends on the coefficient of friction seen by one segment. Thus, for the  $i$ -th component of the fluid we use the ansatz

$$\frac{1}{\tau_{m,i}} \propto g_m(\bar{N})N_i^{-\sigma} \quad (9)$$

where  $g_m(\bar{N})$  is analogous to the internal viscosity function  $g(\bar{N})$ , except now it is for the intermediate time-scale motion. It is expected to have a weaker dependence on  $\bar{N}$  than  $g(\bar{N})$ . For polyethylene and polystyrene melts, the exponent  $\sigma$  was found to be  $\sigma \sim 0.5 \pm 0.3$  [18].

The large scale motion is given by the overall rotation of the molecule (i.e. the lowest rotational mode). The correlation function for this motion should have the usual exponential decay:

$$G_{C,i}(t) = e^{-t/\tau_{R,i}} \quad (10)$$

Then, in the extreme narrowing limit,  $T_{1,i}$  and  $T_{2,i}$  are given by

$$\frac{1}{T_{1,i}} = \frac{1}{T_{2,i}} = C \int G_{B,i}(t)G_{C,i}(t) dt \quad (11)$$

Substituting the expressions of Eqs. (8) and (10) for  $G_{B,i}(t)$  and  $G_{C,i}(t)$  and performing the integral, we obtain

$$\frac{1}{T_{1,i}} = \frac{1}{T_{2,i}} = a\sqrt{\tau_{m,i}\tau_{R,i}} \quad (12)$$

The proportionality factor  $a$  is independent of chain length, friction and internal viscosity. With the expressions for the correlation times  $\tau_{m,i}$  and  $\tau_{R,i}$  given by Eqs. (9) and (7), this equation becomes

$$T_{1,i} = T_{2,i} = a\sqrt{g(\bar{N})g_m(\bar{N})N_i^{-\kappa}} \quad (13)$$

where  $\kappa = (3\nu + \sigma)/2$ . For the values above,  $\kappa = 1.3 \pm 0.15$ . From a fit to alkane data, we found  $\kappa = 1.24$  [16], which we will use throughout. As given in Eq. (5), the internal viscosity function  $g(\bar{N})$  follows a power law in the mean chain length of the mixture. We assume that  $g_m(\bar{N})$  also follows a power-law dependence on the mean chain length, but the dependence ought to be much weaker than the one for  $g(\bar{N})$ . Thus we find that

$$T_{1,i} = T_{2,i} = B\bar{N}^{-\gamma}N_i^{-\kappa} \quad (14)$$

where we expect  $\beta/2 \leq \gamma < \beta$ . For mixtures of alkanes at room temperature and ambient pressure, it was found that  $B = 672$  s and  $\gamma = 1.25$  [16].

## 5. Extracting information about composition from one-dimensional distribution functions

Given the fluid composition, or the chain length distribution  $f(N)$ , Eqs. (6) and (14) can be used to predict the resulting distributions of diffusion coefficients or relaxation times in the fluid. Furthermore, it is possible to invert these relations and infer the chain length distributions  $f(N)$  from the measured distribution functions  $f(D)$ ,  $f(T_1)$  or  $f(T_2)$ . The distribution functions measured by NMR techniques correspond to spin concentrations, whereas the chain length distribution  $f(N)$  extracted from gas chromatography measurements is expressed in weight concentrations. We make here the assumption that the proton spin concentrations are directly proportional to the weight concentrations.

There is an additional subtlety that we have to take into account.  $\bar{N}$  is the molar mean chain length,  $\bar{N} = \sum_i x_i N_i$ , where  $x_i$  is the number density or molar concentration of molecules with chain length  $N_i$ , and not the weight concentration as used for  $f(N)$ . Nevertheless, by making the approximation that the molar weight is proportional to the chain length, we can relate  $\bar{N}$  to  $f(N)$  by  $\bar{N} = [\int f(N)N^{-1} dN]^{-1}$ .

This analysis then shows that a component with diffusion coefficient  $D_i$  corresponds to molecules with a chain length  $N_i$  given by

$$N_i = A^{\frac{1}{\beta+\nu}} \langle D^{\frac{1}{\nu}} \rangle^{\frac{\beta}{\beta+\nu}} D_i^{-\frac{1}{\nu}} \quad (15)$$

where  $\langle D^{\frac{1}{\nu}} \rangle$  is the  $1/\nu$ -th moment of the measured distribution function  $f(\log D)$ :  $\langle D^{\frac{1}{\nu}} \rangle \equiv \int d \log D f(\log D) D^{\frac{1}{\nu}}$ . The resulting distribution of chain lengths is simply related to the measured distribution of diffusion coefficients by

$$f(\log N) = \nu f(\log D) \quad (16)$$

The molar average chain length  $\bar{N}$  can then be calculated from  $f(\log N)$ . Alternatively, it can be directly obtained from the diffusion distribution by

$$\bar{N} = A^{\frac{1}{\beta+\nu}} \langle D^{\frac{1}{\nu}} \rangle^{-\frac{\nu}{\beta+\nu}} \quad (17)$$

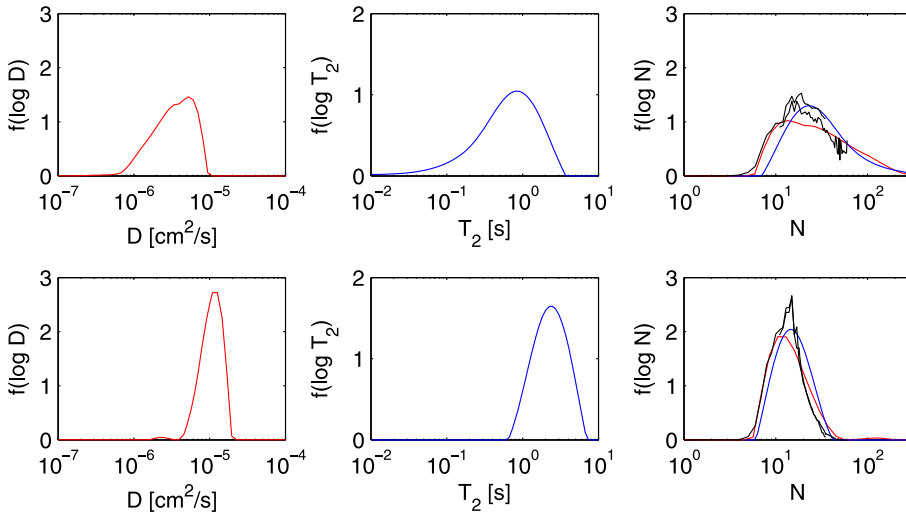


**Fig. 4.** Relation between diffusion and relaxation distribution functions and chain length distributions for two different oils. The panels on the left and in the middle show the measured diffusion distributions  $f(\log D)$  and relaxation distributions  $f(\log T_2)$ , respectively. In the panels on the right, the chain length distributions  $f(\log N)$  inferred from diffusion (red) using Eqs. (15) and (16), and from relaxation (blue) using Eqs. (18) and (19) are compared with those extracted from gas chromatography (black). The oil in the top row has components with more than 60 carbon atoms, which exceeds the range of gas chromatography, even if operated at higher temperatures.

Analogous relations can be obtained for relaxation:

$$N_i = B \frac{1}{\gamma + \kappa} \langle T_2^{\frac{1}{\kappa}} \rangle^{\frac{\gamma}{\gamma + \kappa}} T_{2,i}^{-\frac{1}{\kappa}} \quad (18)$$

and

$$f(\log N) = \kappa f(\log T_2) \quad (19)$$

where  $\langle T_{2,i}^{\frac{1}{\kappa}} \rangle \equiv \int d \log T_2 f(\log T_2) T_2^{\frac{1}{\kappa}}$ . The average chain length  $\bar{N}$  is given by

$$\bar{N} = B \frac{1}{\gamma + \kappa} \langle T_2^{\frac{1}{\kappa}} \rangle^{-\frac{\kappa}{\gamma + \kappa}} \quad (20)$$

In Fig. 4, we compare the chain length distributions of two oils estimated from relaxation and diffusion NMR measurements at low field using Eqs. (15) to (19), with the chain length distributions inferred from gas chromatography measurements. There is good agreement between the width and general shape of  $f(\log N)$ . The gas chromatography data provides higher resolution, but does not extend to the largest molecules. Standard gas chromatography is limited to the analysis of molecules of up to about 36 carbons. When the columns in the gas chromatography apparatus are operated at higher temperature, this limit can be increased to molecules of up to about 60 carbon atoms. Large molecules such as asphaltene cannot be analyzed with gas chromatography. Even though the amount of asphaltene in the oils shown in Fig. 4 is negligible, the oil shown in the top panel contains a sizeable fraction of molecules with more than 60 carbon atoms that can only be directly characterized with the NMR techniques. There is generally good agreement between the concentrations for smaller molecules inferred using the different approaches.

## 6. Temperature dependence

An increase in temperature decreases the viscosity of the fluid and speeds up molecular motions. This leads to an increase in the diffusion coefficients and relaxation times. The temperature dependence of diffusion and relaxation in fluid mixtures has been discussed in [19]. In the absence of phase transitions, the theoretical analysis shows that the general form of the relation between the diffusion coefficients or relaxation times and  $N_i$ , given in Eqs. (4) and (14), is unaffected by temperature. In particular, the exponents  $\nu$  and  $\kappa$  are independent of temperature. This implies that a change in temperature simply rescales the diffusion coefficients or relaxation times by an overall factor that reflects the temperature dependence of the microviscosity. The distribution functions  $f(\log D)$  and  $f(\log T_2)$  are simply shifted along the abscissa, without changing their shape. This behavior is illustrated in Fig. 5 with measured  $T_2$  distribution functions of two oils at four different temperatures. These measurements confirm that to first order the shapes of the distribution functions stay constant.

The temperature induced shifts in diffusion and relaxation times are directly related to the temperature dependence of the microviscosity. In the expression for diffusion, Eq. (4), only the first term has a temperature dependence, i.e.  $g(\bar{N}, T)$ . For mixtures of alkanes, it has been found that this term can be well approximated by

$$g(\bar{N}, T) = A(T) \bar{N}^{-\beta(T)} \quad (21)$$

where at atmospheric pressure  $A(T) = 5.65 \times 10^{-7} \exp\{-\frac{143.7 \text{ K}}{T}\} \frac{\text{m}^2}{\text{s}}$  and  $\beta(T) = \frac{588.5 \text{ K}}{T} - 0.244$ .

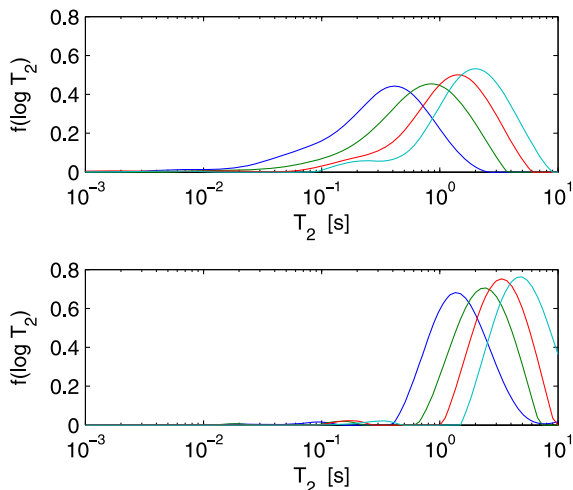


**Fig. 5.** Temperature dependence of  $T_2$  relaxation time distributions for the same two oils shown in Fig. 4. The 4 curves correspond to the distribution functions measured at  $T = 30^\circ, 58^\circ, 86^\circ$  and  $114^\circ\text{C}$ .

Similarly, for relaxation, it was found that expression (14) can be generalized to include the temperature dependence:

$$T_{1,i}(T) = T_{2,i}(T) = B(T)\bar{N}^{-\gamma(T)}N_i^{-\kappa} \quad (22)$$

with  $B(T) = \exp\{\frac{227\text{ K}}{T}\}314\text{ s}$  and  $\gamma(T) = \frac{755\text{ K}}{T} - 1.43$ .

The temperature dependence of the relaxation times can be reformulated in terms of an effective activation energy  $E_{\text{eff}}$ . The relaxation time of a given component at a temperature  $T$ ,  $T_{2,i}(T)$ , is related to that at a reference temperature  $T_0$ ,  $T_{2,i}(T_0)$ , by

$$\frac{T_{2,i}(T)}{T_{2,i}(T_0)} = \exp\left\{-\left(\frac{1}{kT} - \frac{1}{kT_0}\right)E_{\text{eff}}(\bar{N})\right\} \quad (23)$$

where  $E_{\text{eff}}$  has a logarithmic dependence on  $\bar{N}$ :

$$E_{\text{eff}}/k = \frac{d\gamma}{dT^{-1}} \log \bar{N} - \frac{d \log B}{dT^{-1}} \quad (24)$$

With the expressions for  $B(T)$  and  $\gamma(T)$  for alkane mixtures given above, the effective activation energy becomes  $E_{\text{eff}}/k = \log \bar{N}755\text{ K} - 227\text{ K}$ .

In Fig. 6 we plot the first moment of the relaxation time distribution  $f(T_2)$  as a function of the inverse temperature,  $1/T$ , for the two oils shown in Fig. 5. The data follows the form of Eq. (23). The effective activation energy  $E_{\text{eff}}$  can be determined from the slope of this graph. The corresponding values of  $\bar{N}$  are consistent with the results shown in Fig. 4.

This analysis shows that oils with a high average chain length  $\bar{N}$  display a more pronounced temperature dependence for viscosity, relaxation, and diffusion than oils formed from shorter chains. The value of  $\bar{N}$  in an oil often correlates with its viscosity, but there can be exceptions. The viscosity is related to the  $-1$ -th moment of the diffusion distribution,  $\langle D^{-1} \rangle$ . In contrast, the temperature dependence of the viscosity, relaxation time, and diffusion coefficient is controlled by  $\bar{N}$ , which in turn is related to the  $1/\nu$ -th moment of the diffusion distribution (Eq. (17)) or the  $1/\kappa$ -th moment of the relaxation time distribution. It is therefore possible that two oils have identical viscosities at a given temperature, but show different temperature dependence. The measurement of the distribution of diffusion coefficients or relaxation times at a fixed temperature gives enough information to infer both the viscosity and its temperature dependence.

## 7. Complex fluids

The extraction of the chain length distributions from the NMR measurements presented in the previous sections is based on the relations developed originally for mixtures of  $n$ -alkanes. Clearly, the oil samples do not only consist of  $n$ -alkanes. The composition of naturally occurring crude oil is generally complex. In addition to simple chain molecules, they typically

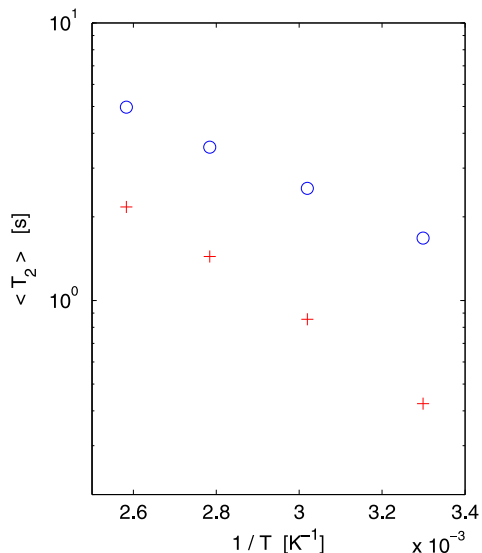


**Fig. 6.** Temperature dependence of the average  $T_2$  relaxation times ( $\langle T_2 \rangle = \int dT_2 T_2 f(T_2)$ ) versus inverse temperature for the two oils shown in Figs. 4 and 5. The effective activation energy  $E_{\text{eff}}$  can be determined from the slope, with the result  $E_{\text{eff}}/k = 1500 \pm 110\text{ K}$  and  $2280 \pm 110\text{ K}$ , respectively. Based on Eq. (24), this corresponds to  $\bar{N} = 9.9 \pm 1.5$  and  $27.6 \pm 4.5$ , which is consistent with the results shown in Fig. 4.



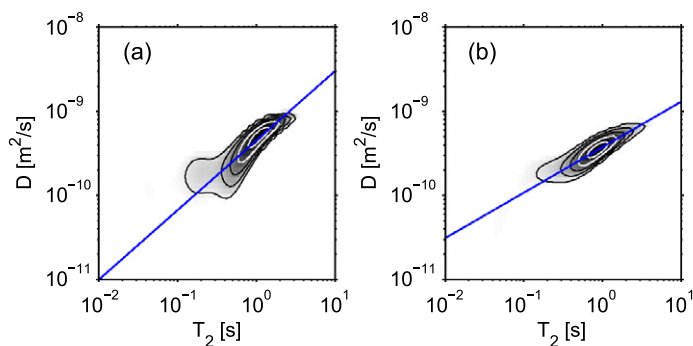


**Fig. 7.** Comparison of two-dimensional distribution functions  $f(\log D, \log T_2)$  for (a) an oil rich in alkanes and (b) an oil rich in aromatics. The straight lines correspond to  $\nu/\kappa = 0.84$  and  $0.55$ , respectively.

also include sizeable fractions of molecules that are branched, that contain double bonds or have aromatic rings. Because alkane molecules are a significant fraction of the composition in many crude oils, the alkane mixture model is a reasonable model. Nevertheless, it is remarkable that the simple scaling relations developed from the analysis of alkane mixtures are so successful in predicting the behavior in these more complex fluids. This suggests that the form of Eqs. (6) and (13) is quite general and captures the essential physics of the problem.

### 7.1. Biodegraded oils with high aromatic content

On closer inspection, we expect that the exponents  $\nu$  and  $\kappa$  are not fully universal and depend somewhat on the chemical composition of the fluids. As an example, aromatic molecules are not as flexible as alkane chains. This will affect the exponent  $\kappa$  and could have an impact on the analysis of biodegraded oils. In these samples, the fraction of aromatic and cyclic molecules is often much more abundant than in regular oils.

The ratio of  $\nu/\kappa$  can be extracted from two-dimensional relaxation–diffusion correlation functions,  $f(\log D, \log T_2)$ . By combining Eqs. (6) and (13), it follows that the diffusion coefficient and relaxation time of each component has a power-law correlation  $D_i \propto T_{2,i}^{\nu/\kappa}$  [20]. Fig. 7 shows measurements of  $f(\log D, \log T_2)$  for two crude oils with contrasting amounts of aromatic components. Both oils show a power-law dependence between the diffusion coefficient and the relaxation time, but the exponent  $\nu/\kappa$  for the biodegraded oil is significantly smaller than for the alkane rich oil. This suggests that the measured value of  $\nu/\kappa$  can be used as an indicator of the chemical composition of the fluid.

### 7.2. Oils with significant asphaltene content

As has been already mentioned at the beginning of this paper, the presence of asphaltene molecules, a common ingredient in many crude oils, strongly affects the relaxation behavior of the fluid. Asphaltene molecules easily aggregate and act as relaxation contrast agents. The asphaltene aggregates form large structures which introduce motion slow compared to the Larmor frequency. The nature of this slow motion can be probed by measurements of two-dimensional  $T_1$ – $T_2$  distribution functions [20]. Fig. 8 shows a typical result of  $f(\log T_1, \log T_2)$  measured at 1.76 MHz for an oil with asphaltene. For all components, the longitudinal relaxation times are longer than the transverse relaxation times,  $T_{1,i} > T_{2,i}$ . This is a clear indicator of the existence of slow motion. Furthermore, it is remarkable that the ratio of  $T_1/T_2$  for all components is rather constant and is not correlated with the relaxation time of the component.

This suggests that the noise fluctuations experienced by component  $i$  have a correlation function of the form  $G_i(t) = G_{c,i}(t)G_{Asph}(t)$ . Here  $G_{Asph}(t)$  represents the slow fluctuations generated by the tumbling of the large asphaltene aggregates that are experienced by all components, and  $G_{c,i}(t)$  represents the fast fluctuations specific to a given component  $i$ . Since the time dependence of  $G_{c,i}(t)$  is fast compared to the Larmor frequency, the low frequency dispersion of the noise spectrum is completely determined by  $G_{Asph}(t)$ , and all components  $i$  have an identical  $T_1/T_2$  ratio. This is consistent with the data in Fig. 8.

A model with these properties has been recently discussed in [21] and used to infer the size of the asphaltene aggregates. It is based on the picture that the fluid contains large porous asphaltene aggregates that tumble slowly in the fluid with a characteristic time scale  $\tau_A$ . The small oil molecules diffuse in the fluid and get temporarily entangled in the asphaltene aggregates. The motion of the entangled oil molecule is highly correlated so that the correlation function  $G_{c,i}(t)$  decays only as a power law with a time constant  $\tau_i$ . The resulting correlation function for the overall motion of the molecules entangled in the slowly tumbling aggregates has then the form  $G_i(t) = (t/\tau_i)^{-d/2} \exp\{-t/\tau_A\}$ , where  $d$  is the dimensionality of the diffusive motion of the oil molecule in the asphaltene aggregate. Within this model, the time scale  $\tau_A$  can be extracted from the measured  $T_1/T_2$  ratio, which in turn can be used to infer the size of the asphaltene aggregates [21].

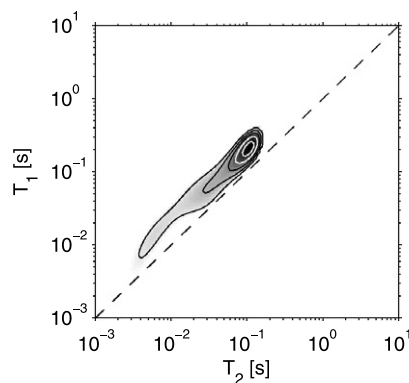


**Fig. 8.** Two-dimensional distribution function  $f(\log T_1, \log T_2)$  for an oil that contains asphaltene. The dashed line indicates  $T_1 = T_2$ . The distribution function for this oil is characterized by a  $T_1/T_2$  ratio that is clearly higher than 1 and approximately constant.

## 8. Conclusion

The molecular dynamics of fluids consisting of a mixture of molecules with a wide range of sizes is complex and involves many different time scales. The relaxation decay typically deviates significantly from an exponential decay. It is therefore generally insufficient to describe the relaxation and diffusion properties with only an average relaxation time or diffusion coefficient. To obtain a detailed understanding of the fluid and its composition, it is essential to analyze the shape of the relaxation decay. We have shown here that it is useful to analyze the relaxation and diffusion behavior in terms of one- and two-dimensional distribution functions. Using simple scaling arguments, we demonstrate that the one-dimensional distribution functions can be directly related to the composition of the fluids, in particular to the distribution of molecular sizes. Furthermore, two-dimensional distribution functions give additional information about the fluid properties, including the presence of supermolecular aggregates and chemical properties.

We have focused in this paper on the study of complex fluid mixtures and shown that the measurement of one- and two-dimensional distribution functions allows us to obtain detailed information about the composition of the sample. Related approaches based on distribution functions have been used for the characterization of many other complex or heterogeneous systems. Examples include the quantification of different immiscible fluids in porous media [22], the characterization of the pore structure of cement [23], or the study of food products [24]. The method is particularly well suited for the noninvasive study of opaque samples and has extended the range of useful NMR applications. Unlike NMR spectroscopy, NMR relaxation and diffusion measurements do not require strong, homogeneous magnetic fields and can be performed with much simpler equipment, including permanent magnets. This has made it possible to perform this NMR modality with unilateral devices where the sample is located outside the measurement device. It has already found widespread application for the characterization of fluids in geological formations using NMR well-logging devices.

## References

- [1] N. Bloembergen, E.M. Purcell, R.V. Pound, Relaxation effects in nuclear magnetic resonance absorption, *Phys. Rev.* 73 (1948) 679–712.
- [2] J. Kowalewski, L. Mäler, *Nuclear Spin Relaxation in Liquids: Theory, Experiments, and Applications*, Taylor & Francis, New York, London, 2006.
- [3] R.L. Grob, E.F. Barry, *Modern Practice of Gas Chromatography*, fourth ed., Wiley-Interscience, 2004.
- [4] A.G. Marshall, Milestones in Fourier transform ion cyclotron resonance mass spectrometry technique development, *Int. J. Mass Spectrom.* 200 (2000) 331–356.
- [5] R.R. Ernst, G. Bodenhausen, A. Wokaun, *Principles of Nuclear Magnetic Resonance in One and Two Dimensions*, Oxford University Press, 1987.
- [6] A. Abragam, *The Principles of Nuclear Magnetism*, Oxford University Press, 1961.
- [7] R. Kimmich, E. Ansaldo, Field-cycling NMR relaxometry, *Prog. Nucl. Magn. Reson. Spectrosc.* 44 (2004) 257–320.
- [8] E.J. Fordham, A. Sezginer, L.D. Hall, Imaging multiexponential relaxation in the  $(y, \log_e T_1)$  plane, with application to clay filtration in rock cores, *J. Magn. Reson. A* 113 (1995) 139–150.
- [9] Y.-Q. Song, L. Venkataraman, M.D. Hürlimann, M. Flaum, P. Frulla, C. Straley,  $T_1$ – $T_2$  correlation spectra obtained using a fast two-dimensional Laplace inversion, *J. Magn. Reson.* 154 (2002) 261–268.
- [10] M.D. Hürlimann, L. Venkataraman, Quantitative measurement of two dimensional distribution functions of diffusion and relaxation in grossly inhomogeneous fields, *J. Magn. Reson.* 157 (2002) 31–42.
- [11] L. Venkataraman, Y.-Q. Song, M.D. Hürlimann, Solving Fredholm integrals of the first kind with tensor product structure in 2 and 2.5 dimensions, *IEEE Trans. Signal Process.* 50 (2002) 1017–1026.
- [12] C. Epstein, J. Schotland, The bad truth about Laplace's transform, *SIAM Rev.* 50 (2008) 504–520.
- [13] M. Prange, Y.Q. Song, Quantifying uncertainty in NMR  $T_2$  spectra using Monte Carlo inversion, *J. Magn. Reson.* 196 (2009) 54–60.
- [14] D.E. Freed, L. Burcaw, Y.-Q. Song, Scaling laws for diffusion coefficients in mixtures of alkanes, *Phys. Rev. Lett.* 94 (2005) 067602.
- [15] M. Doi, S.F. Edwards, *The Theory of Polymer Dynamics*, Oxford University Press, 1998.
- [16] D.E. Freed, Dependence on chain length of NMR relaxation times in mixtures of alkanes, *J. Chem. Phys.* 126 (2007) 174502.
- [17] D.E. Woessner, B.S. Snowden, R.A. McKay, E.T. Strom, Proton and deuteron spin-lattice relaxation in *n*-dodecane, *J. Magn. Reson.* 1 (1969) 105–118.
- [18] R. Kimmich, R. Bachus, NMR field-cycling relaxation spectroscopy, transverse NMR relaxation, self-diffusion and zero-shear viscosity: Defect diffusion and reptation in non-glassy amorphous polymers, *Colloid Polym. Sci.* 260 (1982) 911–936.

- [19] D.E. Freed, Temperature and pressure dependence of the diffusion coefficients and NMR relaxation times of mixtures of alkanes, *J. Phys. Chem. B* 113 (2009) 4293–4302.
- [20] A.R. Mutina, M.D. Hürlimann, Correlation of transverse and rotational diffusion coefficient: A probe of chemical composition in hydrocarbon oils, *J. Phys. Chem. A* 112 (2008) 3291–3301.
- [21] L. Zielinski, I. Saha, D.E. Freed, M.D. Hürlimann, Y. Liu, Probing asphaltene aggregation in native crude oils with low-field NMR, *Langmuir* 26 (2010) 5014–5021.
- [22] M.D. Hürlimann, M. Flaum, L. Venkataramanan, C. Flaum, R. Freedman, G.J. Hirasaki, Diffusion–relaxation distribution functions of sedimentary rocks in different saturation states, *Magn. Reson. Imaging* 21 (2003) 305–310.
- [23] L. Monteilhet, J.-P. Korb, J. Mitchell, P.J. McDonald, Observation of exchange of micropore water in cement pastes by two-dimensional  $T_2$ – $T_2$  nuclear magnetic resonance relaxometry, *Phys. Rev. E* 74 (2006) 061404.
- [24] M.D. Hürlimann, L. Burcaw, Y.Q. Song, Quantitative characterization of food products by two-dimensional  $D$ – $T_2$  and  $T_1$ – $T_2$  distribution functions in a static gradient, *J. Colloid Interface Sci.* 297 (2006) 303–311.